Conformational Analysis of Two Cyclic Analogs of Angiotensin: Implications for the Biologically Active Conformation†

Gregory V. Nikiforovich,*,‡ Jeff L.-F. Kao,§ Krystyna Plucinska,∥,⊥ Wei Jun Zhang,∥ and Garland R. Marshall‡

Center for Molecular Design and Department of Chemistry, Washington University, and Department of Molecular Biology and Pharmacology, Washington University School of Medicine, St. Louis, Missouri 63130

Received November 24, 1993; Revised Manuscript Received January 26, 1994®

ABSTRACT: Conformations of two cyclic analogs of angiotensin (Asp[1]-Arg[2]-Val[3]-Tyr[4]-Val/Ile[5]-His[6]-Pro[7]-Phe[8], AT), *cyclo*[Sar[1], Cys[3], Mpt[5]]-AT and *cyclo*[Sar[1], HCys[3], Mpt[5]]-AT, were studied, independently employing two complementary techniques, energy calculations and NMR measurements in DMSO solution. NMR data were indicative of well-defined solution conformations for the cyclic moieties of *cyclo*[Sar[1], Cys[3], Mpt[5]]-AT and *cyclo*[Sar[1], HCys[3], Mpt[5]]-AT, including the ϕ values for the Cys[3]/HCys[3] and Tyr[4] residues, as well as the χ_1 value for the Tyr[4] residue. Solution conformations for the exocyclic linear parts of both molecules cannot be described by the NMR data with the same precision. At the same time, independent energy calculations revealed the same conformations of cyclic moieties of *cyclo*[Sar[1], Cys[3], Mpt[5]]-AT and *cyclo*[Sar[1], HCys[3], Mpt[5]]-AT among low-energy conformers for both peptides. Moreover, the same conformations are compatible with the model of AT receptor-bound conformation (Nikiforovich & Marshall, 1993), which assumes the particular spatial arrangement of aromatic moieties of Tyr[4], His[6], and Phe[8] residues and the C-terminal carboxyl. These conformers of *cyclo*[Sar[1], Cys[3], Mpt[5]]-AT and *cyclo*[Sar[1], HCys[3], Mpt[5]]-AT contain "an open turn" in the backbone of the Tyr[4]-Val[5] residues, instead of the earlier proposed β-like reversal, thus confirming the suggestion that the conformation(s) ensuring binding of AT analogs with specific receptors should not be described in terms of a unique backbone conformer.

Conformational studies of a well-known pressor and myotropic agent, angiotensin (Asp[1]-Arg[2]-Val[3]-Tyr[4]-Val/Ile[5]-His[6]-Pro[7]-Phe[8], AT), have been very extensive in the past two decades [e.g., see Duncia et al. (1990) and references therein]. These studies yield significantly different models of AT conformation(s) in solution and/or at the receptor surface (receptor-bound conformations). Different authors have suggested that AT structure in solution is close to a random coil (Paiva et al., 1963), an α-helix (Smeby et al., 1962), a structure with ionic-dipole interaction of the (His[6])NH$^+$···$^-$OOC(Phe[8]) type (Weinkam & Jorgensen, 1971), an inverse γ-turn at the Tyr[4] residue with *cis*-conformation of Pro[7] residue, or a β-turn at the Tyr[4]-Val[5] residues (Printz et al., 1972), the so-called cross-β-forms I (Devynck et al., 1973) and II (Fermandjian et al., 1976), a structure with clustering of aromatic rings for His, Tyr, and Phe residues (Matsoukas et al., 1990), or a state of dynamic equilibrium between two main forms with a β-turn either at the Val[3]-Tyr[4] or Tyr[4]-Val[5] residues (Nikiforovich et al., 1988). As a receptor-bound conformation of AT, different studies have proposed a β-III-like turn at the Tyr[4]-Val[5] residues (Balodis & Nikiforovich, 1980; Chipens et al., 1979; Marshall, 1986), a model where hydroxyl group of Tyr[4] side chain is placed close to the C-terminal carboxyl (Turner et al., 1991), and, recently, a model pointing out the importance of a common spatial arrangement of aromatic moieties of Tyr[4], His[6], and Phe[8] residues, as well as the C-terminal carboxyl (which are the functional groups triggering biological response of AT), rather than of any particular backbone structures (Nikiforovich & Marshall, 1993).

One of the main reasons for such a variety of conformational models for AT is due to conformational flexibility of the angiotensin molecule, which is a linear octapeptide. The way to distinguish among possible conformational models for AT, especially those for receptor-bound conformers, is to design conformationally constrained (e.g., cyclic) analogs retaining high levels of binding to specific receptors. Several such attempts failed (De Coen et al., 1975; Miranda & Juliano, 1988), but, recently, one particular type of cyclic AT analog has been found to possess high affinity toward specific receptors (Plucinska et al., 1993; Spear et al., 1990; Sugg et al., 1989). This type of analog involves the formation of disulfide bridge between positions 3 and 5 in the AT sequence and is exemplified by *cyclo*[HCys/Cys[3],HCys[5]]-AT [IC_{50} = 2.1 and 13 nM at rat uterine membrane, respectively (Spear et al., 1990)] or *cyclo*[Sar[1], HCys/Cys[3], Mpt[5]]-AT [IC_{50} = 0.65 and 0.82 nM at rabbit uterus, respectively (Plucinska et al., 1993)], where Mpt is *trans*-4-mercaptoproline. The central fragment for both kinds of such analogs contains a cyclic moiety, which is certainly less flexible in the case of *cyclo*[Sar[1], HCys/Cys[3], Mpt[5]] analogs due to an additional conformational constraint ($\phi_5 \approx -60°$) imposed by the mercaptoproline ring. Besides, the $C^\delta H_2$ atomic center of the same ring (i.e., an N-methyl residue in position 5) creates an additional steric hindrance, which limits the allowed values of the ψ_4 dihedral angle. Thus, it may be expected that the conformational analysis performed for *cyclo*[Sar[1], HCys/Cys[3], Mpt[5]] analogs of AT will significantly narrow the scope of their possible receptor-bound structures, especially in the central molecular fragment. In this study, we independently employed two complementary techniques, energy calculations and NMR measurements, for this purpose.

† Supported in part by the NIH Grant GM 24483.
* Address correspondence to this author.
‡ Center for Molecular Design.
§ Department of Chemistry.
∥ Department of Molecular Biology and Pharmacology.
⊥ Present address: Institute of Chemistry, University of Gdansk, 80-952 Gdansk, Poland.
® Abstract published in *Advance ACS Abstracts,* March 1, 1994.

0006-2960/94/0433-3591$04.50/0

MATERIALS AND METHODS

NMR Spectroscopy. The peptides, *cyclo*[Sar^1, HCys/Cys^3, Mpt^5] analogs of AT, were prepared and purified exactly as in the earlier paper (Plucinska et al., 1993). Sample was made by dissolving 8 mg of peptide in approximately 0.7 mL of DMSO-d_6. Samples were degassed by several freeze–thaw cycles and sealed in NMR tubes under vacuum. All 2D NMR spectra were recorded with a Varian Unity-600 spectrometer operating at 600 MHz, interfaced with a Sun SPARC I computer. The data were processed off-line on a SPARC 10 station with VNMR software. Chemical shifts were measured in parts per million (ppm) downfield from internal TMS.

The total correlation (2D HOHAHA) spectra (Bax & Davis, 1985) were recorded using an MELV-17 mixing sequence of 120 ms, flanked by two 2-ms trim pulses. Phase-sensitive 2D spectra were obtained by employing the hypercomplex method. A total of 2 × 256 × 1024 data matrix with 16 scans per t_1 value were collected. Gaussian line broadening and sine-bell function were used in weighting t_2 and t_1 dimension, respectively. After two-dimensional Fourier transform, the spectra resulted in 1K × 1K data points and were phase and baseline corrected in both dimensions.

The spin-lock NOE (ROESY) spectra (Bax & Davis, 1985; Kessler et al., 1987) resulted from a 2 × 256 × 1024 data matrix with 32 scans per t_1 value. The spectra were recorded with a 200-ms mixing (spin-lock) time. The carrier frequency was positioned at the center of the spectrum, and a 2-kHz rf field strength was used. The hypercomplex method was used to yield phase-sensitive spectra. The data were processed similar to the way in which the 2D HOHAHA spectrum was processed.

The temperature dependencies of the amide proton resonances were determined by six measurements over a range of 25–50 °C.

Energy Calculations. The methods for conformational search and energy calculations were the same as described previously for other peptides (Nikiforovich et al., 1991). The ECEPP/2 potential field (Dunfield et al., 1978; Nemethy et al., 1983) was used for conformational energy calculations assuming rigid valence geometry with planar *trans*-peptide bonds (both *trans* and *cis* peptide bonds were examined for Mpt residues). The ω angles were allowed to vary only inside the cyclic moieties. Since the task of conformational search in this case is to sample thermodynamically stable conformers of the molecule, not to describe energy barriers between them, the assumption of rigid valence geometry seems quite adequate [see also Roterman et al. 1989)]. The valence geometry and atomic charges for the Mpt residue were calculated by the use of the SYBYL program with the standard TRIPOS force field. Aliphatic and aromatic hydrogens were generally included in united atomic centers of CH_n type; H^α atoms and amide hydrogens were described explicitly. The main calculation scheme consisted of a buildup procedure of stepwise successive "growing" of the peptide chain starting from the cyclic moiety in fragment 3–5 to fragment 3–8, then to fragment 2–8, and finally to the entire molecule. At the first step of the calculations, all possible combinations of local minima for the peptide backbone for each amino acid residue were considered, as well as all possible rotamers (g^+, t, and g^-) for side chain dihedral angles χ_1 (Cys^3) and χ_1, χ_2 (HCys^3). Generally, these minima were of *E, F, C, A,* and *A** types [according to the notation in Zimmerman and Scheraga (1977)]. The same minima were considered for Arg^2 and His^6 residues at the subsequent steps. For Pro^7 and Mpt^5 residues, only minima of *F, C,* and *A* types were considered, and, for the terminal residues Sar^1 and Phe^8, there were minima of *E, E*, A,* and *A** types and of *E, A,* and *A** types, respectively. The backbone structures selected at the previous step by $E - E_{min} < \Delta E = 10$ kcal/mol criterion were considered for subsequent steps of the buildup procedure. Also, only structures differing by more than 40° in at least one value of any backbone dihedral angle were selected for the next step. The dihedral angle values of side chain groups (except χ_1 angles for Cys/HCys^3 residues) and of the terminal groups of the backbone were optimized at every step before energy minimization to achieve their most favorable spatial arrangements according to an algorithm previously described (Nikiforovich et al., 1991).

Geometric Comparison for a Pair of Conformers. Geometric similarity for a pair of conformers belonging to different molecules was estimated by an assessment of the best fit of the spatial arrangement for the atomic centers chosen to represent a fragment bearing the important functional groups of AT molecule, namely, the C^β atom for Tyr^4 residue, C^α and C^β atoms for Val^5–Phe^8 residues, and the carbonyl carbon atom of the C-terminal carboxyl. Two conformers were regarded as geometrically similar when the corresponding rms value was less than 1.0 Å.

RESULTS

NMR Measurements. Proton chemical shifts of *cyclo*[Sar^1, HCys^3, Mpt^5]-AT were assigned completely by analysis of HOHAHA and ROESY spectra (Figures 1 and 2, respectively). The Arg^2 residue was identified first by the spin propagation from NH through δH. The correlated proton resonances at 2.1–2.8 ppm were unambiguously assigned to β and γ protons of the HCys^3 residue (Figure 1). Sequential assignment of *cyclo*[Sar^1, HCys^3, Mpt^5]-AT was obtained by using the NH–αH fingerprint region of the ROESY spectrum (Figure 2a). All the $d_{\alpha N}$ connections between adjacent residues were observed, and the segment from Sar^1 to Tyr^4 is explicitly indicated by a continuous path. For the Mpt^5 and Pro^7 residues, the losses of connectivity were restored by NOE's between Tyr^4 α and Mpt^5 δ protons, and between His^6 α and Pro^7 δ protons (Figure 2b). It was, therefore, possible to assign all resonances to specific protons for each residues of *cyclo*[Sar^1, HCys^3, Mpt^5]-AT. The strategy for the assignment of cyclo[Sar^1, Cys^3, Mpt^5]-AT was the same as for *cyclo*[Sar^1,HCys^3,Mpt^5]-AT. Complete assignments for each residues of *cyclo*[Sar^1, HCys^3, Mpt^5]-AT and *cyclo*[Sar^1, Cys^3, Mpt^5]-AT are shown in Table 1.

Interestingly, it was found that the chemical shift differences for the two Mpt^5 δ protons are quite large for both *cyclo*[Sar^1, Cys^3, Mpt^5]-AT ($\Delta\delta$ = 0.6 ppm) and *cyclo*[Sar^1, HCys^3, Mpt^5]-AT ($\Delta\delta$ = 0.3 ppm). Generally, a small chemical shift difference (less than 0.1 ppm) is observed in the δ protons of proline ring in a linear peptide. This occurs because the flexible heterocyclic five-membered ring of proline and the flexible peptide backbone tend to average out anisotropy effects of the carboxyl group in the adjacent peptide bond (Deslauriers et al., 1974). The larger chemical shift difference observed in the Mpt^5 δ protons of *cyclo*[Sar^1, Cys^3, Mpt^5]-AT can be accounted for by the more rigid conformation of the peptide in the 10-membered ring. Furthermore, the bulky disulfide bond and the five-membered ring of the Mpt^5 residue incorporated in the central cyclic fragment of residues 3–5 tend to limit backbone flexibility and force the carboxyl groups away from the 10-membered ring. As a consequence of this, one of the Mpt^5 δ protons is fixed in the shielding zone due to the difference in orientation of these two δ protons with

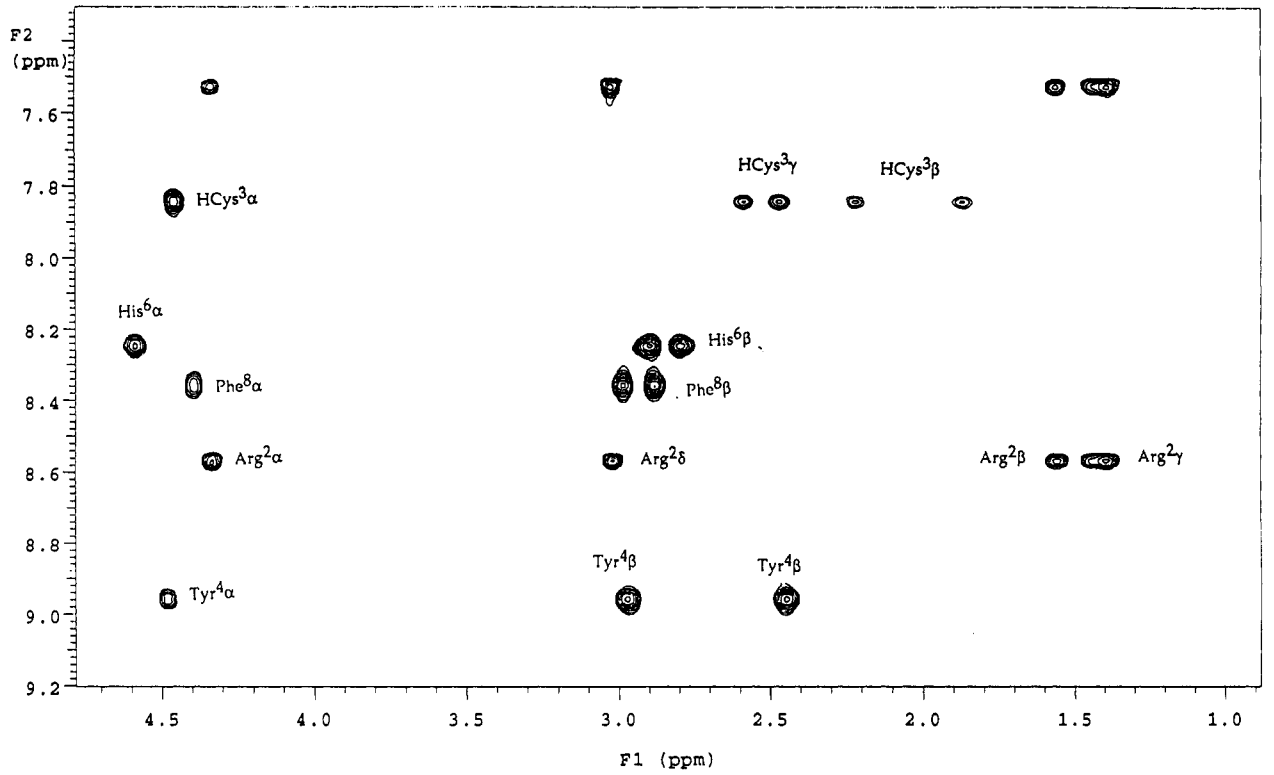

FIGURE 1: Expansion of the NH–αH region of the phase-sensitive 600-MHz 2D HOHAHA spectra of *cyclo*[Sar¹, HCys³, Mpt⁵]-AT. The sample is ~5 mM in DMSO-d_6. A 6000-Hz spectral width in F_2 was collected into 2K data points. A 2 × 256 × 2048 data matrix with 16 scans per t_1 value was acquired within 10 h.

Table 1: Proton Chemical Shifts (ppm) for *cyclo*[Sar¹, HCys³, Mpt⁵]-AT and *cyclo*[Sar¹, Cys³, Mpt⁵]-AT in DMSO-d_6

	cyclo[Sar¹, HCys³, Mpt⁵]-AT				*cyclo*[Sar¹, Cys³, Mpt⁵]-AT			
	NH	αH	βH	others	NH	αH	βH	others
Arg²	8.59	4.33	1.55, 1.42	γ1.39; δ3.02	8.51	4.25	1.43, 1.31	γ1.24, 1.22; δ2.88
HCys³	7.87	4.48	2.20, 1.82	γ2.46, 2.59				
Cys³					7.85	4.32	3.53, 2.79	
Tyr⁴	8.96	4.53	2.94, 2.42		8.84	4.68	2.77, 2.45	
Mpt⁵		4.32	2.07, 1.96	γ3.52; δ3.63, 3.35		4.2	1.82, 1.77	γ3.44; δ3.90, 3.30
His⁶	8.32	4.62	2.90, 2.81		8.14	4.26	2.84, 2.75	
Pro⁷		4.29	1.91, 1.70	γ1.69; δ3.48, 3.31		4.17	1.81, 1.60	γ3.44; δ3.37, 3.23
Phe⁸	8.32	4.39	2.98, 2.88		8.26	4.56	2.82, 2.70	

respect to the carboxyl group of neighboring residues (especially the Tyr⁴ residue), which leads to a strong nonequivalence. In the case of *cyclo*[Sar¹, Cys³, Mpt⁵]-AT, it might be suggested that the side chain rotamers of Tyr⁴ could play a role in this nonequivalence. However, such a large chemical shift difference was also found in rigid peptides, such as *cyclo*-(L-Pro-L-Pro-D-Pro) (Kessler et al., 1982), in which the anisotropy effect of the neighboring carbonyl group contributed to a 0.6 ppm shift change between the δ protons of the proline. This is consistent with the rotamer analysis of the Tyr⁴ side chains (see below), in which the most populated conformation of χ_1 (g^-) places the aromatic ring at the distance of more than 4.5 Å from the Mpt⁵ δ-protons, thus ruling out the ring current effect contributing significantly to the nonequivalence of the Mpt⁵ δ protons. As the ring size increases from *cyclo*[Sar¹, Cys³, Mpt⁵]-AT to *cyclo*[Sar¹, HCys³, Mpt⁵]-AT, the less rigidity of the peptide backbone conformation in the 11-membered ring is reflected in the decrease of nonequivalence of the Mpt⁵ δ protons by half (from 0.6 to 0.3 ppm). A similar observation was also found in the β protons of residue 3, which has an nonequivalence of 0.7 ppm in *cyclo*[Sar¹, Cys³, Mpt⁵]-AT and drops to 0.38 ppm in *cyclo*[Sar¹, HCys³, Mpt⁵]-AT.

The temperature dependences of the amide protons show no evidence of strong intramolecular hydrogen bonds either in *cyclo*[Sar¹, Cys³, Mpt⁵]-AT or in *cyclo*[Sar¹, HCys³, Mpt⁵]-AT. The $\Delta\delta/\Delta T$ values of 4.0–4.5 × 10^{-3} ppm/K obtained for the amide protons of the residues 3, 6, and 7 indicate that these are solvent-exposed NH's, whereas the smaller $\Delta\delta/\Delta T$ values, of 2.2–2.8 × 10^{-3} ppm/K, observed for the Arg² and Tyr⁴ residues, indicate that these amide protons are somewhat shielded from solvent (Table 2). Furthermore, strong NOEs between Tyr⁴ NH and β protons of the residue 3 (Cys³ in *cyclo*[Sar¹, Cys³, Mpt⁵]-AT or HCys³ in *cyclo*[Sar¹, HCys³, Mpt⁵]-AT) and a transannular NOE between HCys³ γ and Mpt⁵ δ protons were observed in the ROESY experiment (Figure 2b). All sequential $d_{\alpha N}$ and $d_{\alpha\delta}$ NOEs (residues 5 and 7) were observed, thus indicating that all proline-preceding amide bonds appear to be in the *trans* conformation. This is consistent with the result that indicated the carbonyl groups in the central cyclic 10/11-membered moieties are pointed out toward the solvent, and the amide proton of Tyr⁴ is partially shielded from the solvent by the relative proximity of the residues in the central cyclic fragment.

Energy Calculations. The buildup procedure found 1331 different low-energy backbone conformers for *cyclo*[Sar¹, Cys³,

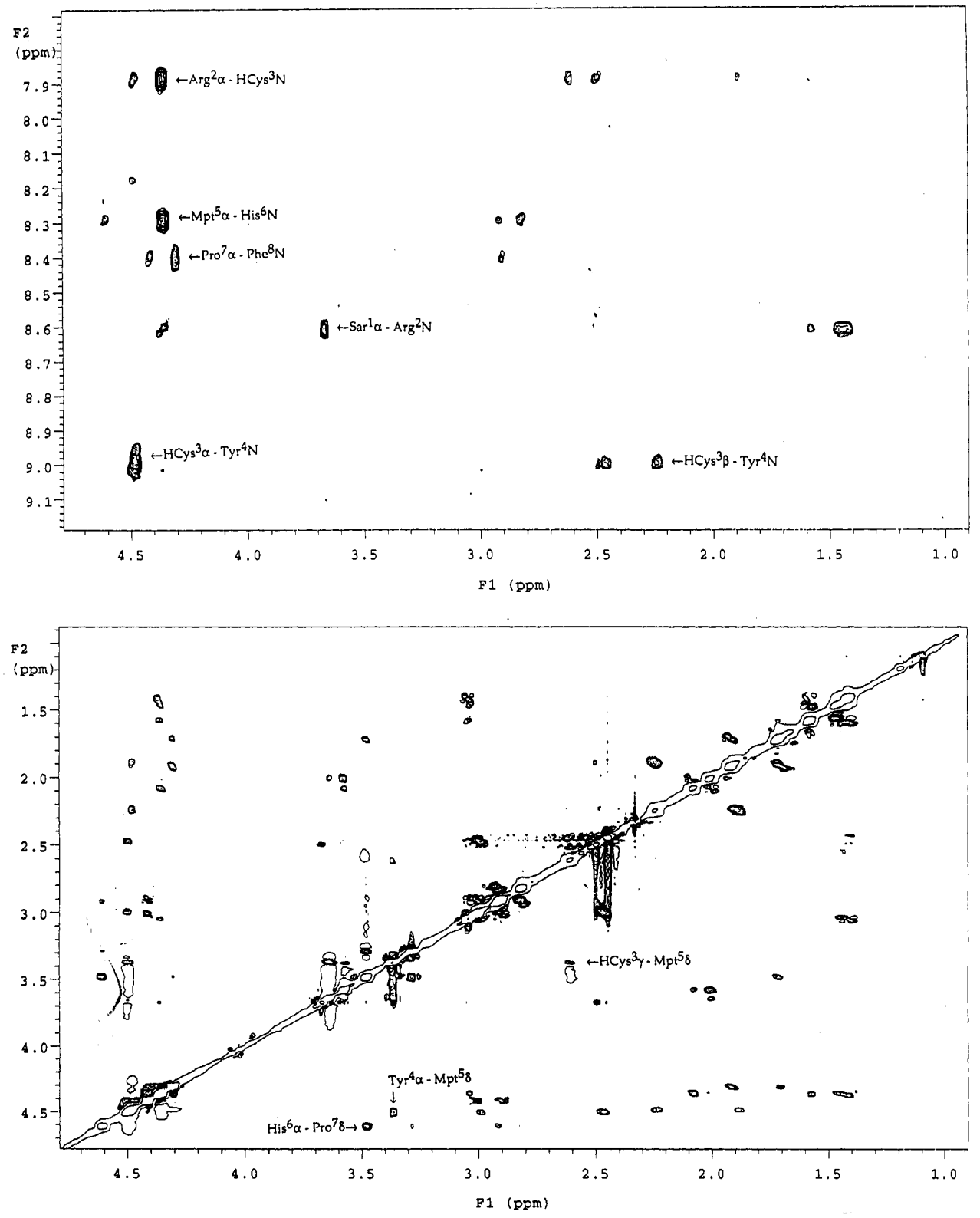

FIGURE 2: Expansions of (a, top) NH–αH, and (b, bottom) aliphatic regions of the 600-MHz 2D ROESY spectra of *cyclo*[Sar^1, HCys^3, Mpt^5]-AT in DMSO-d_6. The NOE cross-peaks were distinguished from scalar-correlated cross-peaks by their negative character.

Mpt^5]-AT and 395 for *cyclo*[Sar^1, HCys^3, Mpt^5]-AT (Table 3), which indicate a quite reasonable conformer sampling for peptides of such size. At first glance, one might see some inconsistency in these results, since a more constrained *cyclo*[Sar^1, Cys^3, Mpt^5]-AT analog possesses a larger number of low-energy structures than the less constrained *cyclo*[Sar^1, HCys^3, Mpt^5]-AT. The data of Table 3 show that, indeed, at the first step of the calculations, the cyclic moiety of the more constrained *cyclo*[Sar^1, Cys^3, Mpt^5]-AT has fewer conformational possibilities than that of the less constrained *cyclo*[Sar^1, HCys^3, Mpt^5]-AT (24 vs 33 low-energy backbone structures, respectively). However, when the cyclic moieties are flanked by the Arg^2 residue and the His^6-Pro^7-Phe^8 fragment, the ratio of accessible structures for cyclic moieties inside low-energy conformers for fragments 2–8 became different, namely, 15 vs 12 structures for *cyclo*[Cys^3, Mpt^5]- and *cyclo*[HCys^3, Mpt^5]-AT$_{2-8}$, respectively. The reason for this is that the slightly more flexible *cyclo*[HCys^3, Mpt^5]

Table 2: Vicinal Constant $J_{NH\alpha H}$ and $J_{\alpha\beta}$ Values (Hz), Temperature Dependences of Chemical Shifts for Amide Protons (10^{-3} ppm/K), and the Tyr[4] Side Chain Populations for *cyclo*[Sar[1], HCys[3], Mpt[5]]-AT and *cyclo*[Sar[1], Cys[3], Mpt[5]]-AT in DMSO-d_6

	cyclo[Sar[1], HCys[3], Mpt[5]]-AT			*cyclo*[Sar[1], Cys[3], Mpt[5]]-AT		
	$J_{NH-\alpha H}$	$\Delta\delta/\Delta T$	side chains	$J_{NH-\alpha H}$	$\Delta\delta/\Delta T$	side chains
Arg[2]	7.3	2.8		8.0	2.3	
HCys[3]	6.9	4.6				
Cys[3]				6.9	4.4	
Tyr[4]	9.3	2.7	$J_{\alpha\beta}$ = 6.3; 9.0 g$^-$ ≈ 59%, t ≈ 41%	9.9	2.2	$J_{\alpha\beta}$ = 6.0, 8.9 g$^-$ ≈ 63%, t ≈ 37%
His[6]	7.8	4.3		8.0	4.2	
Phe[8]	7.8	4.0		7.6	4.3	

Table 3: Buildup Procedure of Energy Calculations for Cyclic Analogs of AT

compound	sequence	structures considered	structures selected
cyclo[Sar[1], Cys[3], Mpt[5]]-AT	Ac-Cys-Tyr-Mpt-NMe	450	24
	Ac-Cys-Tyr-Mpt-His-Pro-Phe	1575	345
	Ac-Arg-Cys-Tyr-Mpt-His-Pro-Phe	1725	345
	Sar-Arg-Cys-Tyr-Mpt-His-Pro-Phe	1380	1331
cyclo[Sar[1], HCys[3], Mpt[5]]-AT	Ac-HCys-Tyr-Mpt-NMe	1350	33
	Ac-HCys-Tyr-Mpt-His-Pro-Phe	1485	308
	Ac-Arg-HCys-Tyr-Mpt-His-Pro-Phe	1540	117
	Sar-Arg-HCys-Tyr-Mpt-His-Pro-Phe	468	395

Table 4: Different Structures of the Fragment 3–5 Found in Low-Energy Conformers of *cyclo*[Sar[1], Cys[3], Mpt[5]]-AT and *cyclo*[Sar[1], HCys[3], Mpt[5]]-AT

		Cys/HCys		Tyr			Pro			
compound	no.	ϕ_3	ψ_3	ω	ϕ_4	ψ_4	ω	ψ_5	energy (kcal/mol)	no. conf.
[Sar[1], Cys[3], Mpt[5]]-AT	1	−76	141	169	−134	55	−160	−11	2.50	305
	2	−155	166	171	−131	56	−155	−13	3.55	199
	3	−156	165	171	−130	56	−155	157	4.11	131
	4	−60	154	173	−125	55	−152	142	4.24	233
	5	−155	167	171	−131	55	−154	99	5.31	124
	6	−60	149	−171	−76	−22	−64	−7	5.40	50
	7	−71	−55	−170	33	61	−176	−4	5.86	67
	8	−92	137	171	−133	55	−161	71	6.56	178
	9	68	145	167	−138	55	−158	−12	7.65	15
	10	−64	152	−171	−81	−20	−66	110	10.33	8
	11	−84	−60	−173	39	55	−167	140	10.81	7
	12	−159	160	−173	−86	−20	−67	−7	11.26	3
	13	−125	2	−163	33	57	−163	−10	11.49	4
	14	−84	−60	−173	39	56	−168	76	11.75	6
	15	−154	165	−171	−105	−10	−80	81	12.48	1
[Sar[1], HCys[3], Mpt[5]]-AT	1	−94	145	176	−135	67	−164	−12	−1.83	104
	2	−145	−62	−173	45	69	−171	−7	1.20	42
	3	−96	−59	−171	40	72	−174	70	1.22	42
	4	−156	141	180	−140	65	−161	−13	1.27	36
	5	−101	87	164	−130	71	−177	66	2.34	4
	6	−71	−45	−171	41	66	−177	−6	2.83	42
	7	−85	147	172	−134	68	−164	153	4.97	41
	8	−84	147	171	−132	72	−174	71	5.50	42
	9	−148	−63	−170	43	76	174	60	5.72	23
	10	−148	109	176	−144	63	−168	70	5.99	4
	11	−154	104	180	−137	61	−163	131	6.01	4
	12	−150	−60	−179	45	62	−157	149	6.48	11

moiety allows the flanking residues to interact more effectively than in the case of the more rigid *cyclo*[Cys[3], Mpt[5]] moiety. As a result of this interaction, some structures of the cyclic moiety inside *cyclo*[Sar[1], HCys[3], Mpt[5]]-AT become stabilized significantly more than others, whereas for *cyclo*[Sar[1], Cys[3], Mpt[5]]-AT the corresponding stabilization is more uniform over the initial cyclic moiety structures. Therefore, less low-energy conformers fit into a given gap for relative energy (ΔE = 10 kcal/mol) in the case of *cyclo*[Sar[1], HCys[3], Mpt[5]]-AT than in the case of *cyclo*[Sar[1], Cys[3], Mpt[5]]-AT. Still, 12 different conformational types of the cyclic moiety backbone can be found among 395 low-energy conformers for *cyclo*[Sar[1], HCys[3], Mpt[5]]-AT, and 15 different types among 1331 low-energy conformers for *cyclo*[Sar[1], Cys[3], Mpt[5]]-AT. The dihedral angle values of fragment 3–5 corresponding to the lowest energy conformers for each of these conformational types are listed in Table 4 for both analogs.

Data of Table 4 show that conformers for the central fragments 3–5 differ mostly in their ϕ_3 and ψ_5 values, i.e., by dihedral angles outside the cycles. As to dihedral angle values inside the cycles, the Tyr[4] residue in *cyclo*[Sar[1], HCys[3], Mpt[5]]-AT possesses only two types of backbone structures, namely, those with $\phi_4 \approx -135°$, $\psi_4 \approx 70°$ [conformation of *D* type (Zimmerman & Scheraga, 1977); structures 1, 4, 5, 7, 8, 10, and 11 in Table 2] and with $\phi_4 \approx 45°$, $\psi_4 \approx 70°$ [conformation of *A** type (Zimmerman & Scheraga, 1977); structures 2, 3, 6, 9, and 12 in Table 2]. The former conformation of Tyr[4] was found in 235 out of 395 low-energy structures of *cyclo*[Sar[1], HCys[3], Mpt[5]]-AT, and the latter was found in 160 structures. Interestingly, the Tyr[4] conformations of *D*

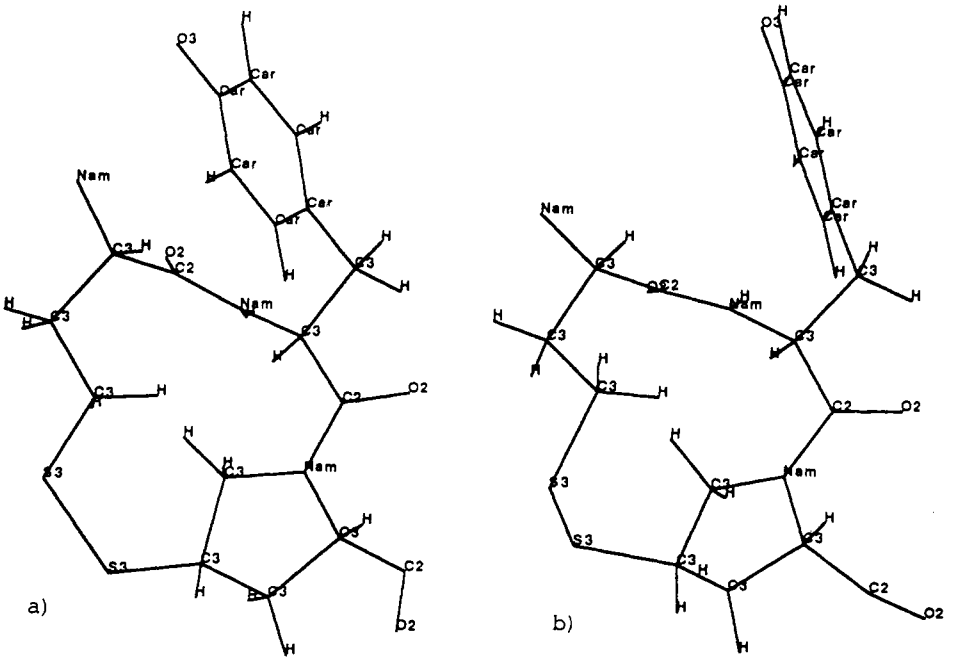

FIGURE 3: Solution conformations of cyclic moiety in *cyclo*[Sar^1, HCys^3, Mpt^5]-AT deduced by NMR data (a) and by energy calculations consistent with NMR data (b).

type appear in Table 4 always in conjunction with positive values of ψ_3 for HCys^3, and conformations of A^* type require negative values of this angle (Table 4). These two options correspond basically to the same geometrical form of the cycle structure, differing mainly by rotation of the HCys^3–Tyr^4 peptide bond plane. It should be noted also that ω angle values inside the cyclic moiety of *cyclo*[Sar^1, HCys^3, Mpt^5]-AT are rather close to the *trans* conformation. For *cyclo*[Sar^1, Cys^3, Mpt^5]-AT, conformation of D type for the Tyr^4 residue became highly predominant (found in 1185 out of 1331 conformers; structures 1, 2, 3, 4, 5, 8, and 9 in Table 4), whereas conformation of A^* type occurs only in 84 conformers (structures 7, 11, 13, and 14 in Table 4). The values of the ψ_3 dihedral angle depend on conformations D and A^* of the Tyr^4 residue in *cyclo*[Sar^1, Cys^3, Mpt^5]-AT in exactly the same manner, as in *cyclo*[Sar^1, HCys^3, Mpt^5]-AT. However, there are two more possible conformations of the Tyr^4 residue for *cyclo*[Sar^1, Cys^3, Mpt^5]-AT, namely, A (61 conformers; structures 6, 10, and 12 in Table 4) and B (one conformer; structure 15 in Table 4). Both of them are incompatible with *trans* peptide bonds inside the cyclic moiety, which leads to a distortion of the ω angle between Tyr^4 and Mpt^5 at the range of 60°–80° (Table 4).

DISCUSSION

Possible Solution Conformations Deduced by NMR. The backbone conformations of *cyclo*[Sar^1, Cys^3, Mpt^5]-AT and *cyclo*[Sar^1, HCys^3, Mpt^5]-AT were examined by correlating the values of the coupling constants $J_{HN-\alpha H}$ with possible dihedral angles ϕ using the angular dependence of coupling constant with the Bystrov parametrization (Bystrov, 1976). The vicinal coupling constants for residues 3–5 in the cyclic moiety indicate that there are four possible values for ϕ angles: ϕ_4 from −140° to −160° and from −90° to −110°, and ϕ_3 from −150° to −170° and from −70° to −90° (Table 2). However, only the values ϕ_4 from −140° to −160° and ϕ_3 from −70° to −90° are consistent with the model building. Only in such a case can the cyclic fragment of residue 3–5 be closed through a disulfide bond with the correct bond length of 2.04 ± 0.40 Å, the backbone conformation of the Tyr^4 residue being of the D type. Moreover, such ring closure brings the Tyr^4 NH and the Cys^3/HCys^3 βH, as well as the HCys^3 γH and the Mpt^5 δH in close proximity (≤3.0 Å), thus meeting the NOE criteria. Residues outside the central cyclic fragment all show strong sequential $d_{\alpha N}$ NOEs, and all have the values of $J_{HN-\alpha H}$ ~8 Hz, indicating that peptide backbone in these regions is in the extended or random-coil conformation (Pardi et al., 1984; Wüthrich et al., 1984).

The rotamer population for the Tyr^4 residue was calculated using the best fit for the values of the coupling constant $J_{\alpha H-\beta H}$ (de Leeuw & Altona, 1982). The g$^-$ and t rotamers constituted the most dominate population (Table 2). The g$^+$ rotamer is sterically unfavorable due to interactions between the aromatic ring of Tyr^4 and the bulky disulfide bond and five-membered ring of Mpt^5. The g$^-$ rotamer may constitute up to 70% of the population, which places the Tyr^4 aromatic ring in the region near residues 2 and 3 . The result is consistent with the temperature coefficient obtained for chemical shift of the amide proton of the Arg^2 residue, in which the NH may be partially shielded from the solvent due to the nearby aromatic ring of the Tyr^4.

Finally, it may be summarized that NMR data are indicative of the well-defined solution conformation for the cyclic moieties of *cyclo*[Sar^1, Cys^3, Mpt^5]-AT and *cyclo*[Sar^1, HCys^3, Mpt^5]-AT, including the ϕ values for the Cys^3/HCys^3 and Tyr^4 residues (D type backbone conformation), as well as the χ_1 value for the Tyr^4 residue (Figure 3a). Solution conformations for the exocyclic linear parts of both molecules cannot be described with the same precision.

Possible Solution Conformation Models by Energy Calculations. On the other hand, one can construct models of *cyclo*[Sar^1, HCys^3, Mpt^5]-AT and *cyclo*[Sar^1, Cys^3, Mpt^5]-AT conformations in solution comparing the data on low-energy conformers in Table 4 with the experimental NMR data in Table 2. Due to the large number of low-energy backbone conformers predicted for the entire *cyclo*[Sar^1, HCys^3, Mpt^5]-AT and *cyclo*[Sar^1, Cys^3, Mpt^5]-AT molecules by calculations, any single model of solution conformation(s) for entire molecule would necessary be the result of conformational averaging over all 395 or 1331 backbone conformers,

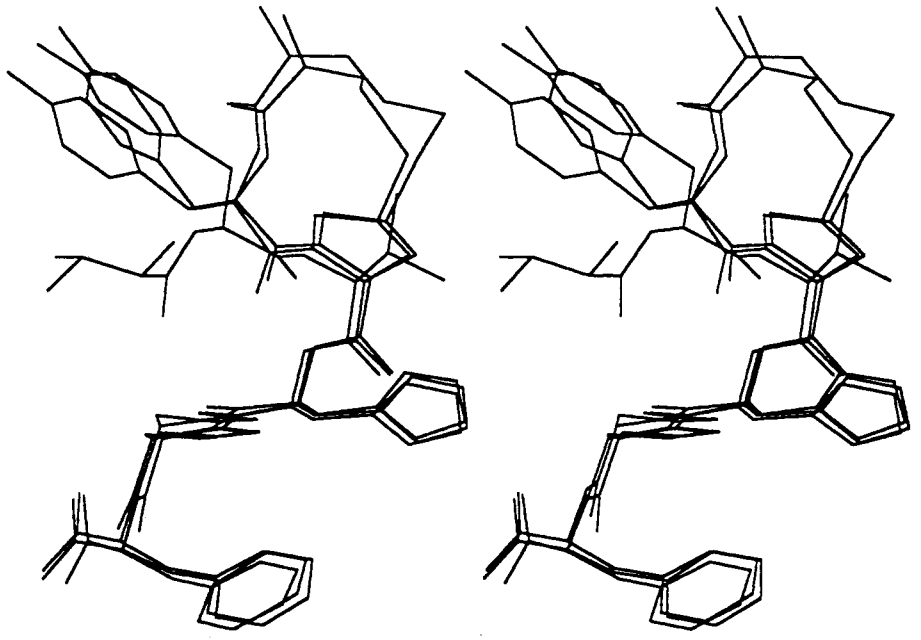

FIGURE 4: Stereoview of AT conformer overlapped on compatible *cyclo*[Sar^1, HCys^3, Mpt^5]-AT and *cyclo*[Sar^1, Cys^3, Mpt^5]-AT conformers from Table 6. Only 3–8 fragments are shown. All hydrogen atoms are omitted.

Table 5: Limits of $J_{NH\alpha H}$ Values (Hz) Calculated for Low-Energy Conformers of *cyclo*[Sar^1, HCys^3, Mpt^5]-AT and *cyclo*[Sar^1, Cys^3, Mpt^5]-AT Consistent with NMR Data

cyclo[Sar^1, HCys^3, Mpt^5]-AT			*cyclo*[Sar^1, Cys^3, Mpt^5]-AT		
structure no.	HCys	Tyr	structure no.	Cys	Tyr
1	5.8–9.7	6.9–10.0	1	3.2–8.0	7.0–10.0
4	4.4–8.8	6.4–9.9	2	4.6–8.9	7.3–10.0
5	6.5–10.0	7.3–9.9	3	4.4–8.8	7.3–9.9
7	4.6–8.9	7.0–10.0	5	4.6–8.9	7.3–10.0
8	4.4–8.8	7.2–10.0	8	5.6–9.5	7.1–10.0
10	5.6–9.5	6.0–9.8	9	4.9–7.9	6.6–10.0
11	4.7–9.0	6.7–10.0	15	4.7–9.0	6.9–10.0
experiment	6.9	9.3	experiment	6.9	9.9

respectively (see Table 3). At the same time, the limited numbers of low-energy conformers in Table 4 make it possible to calculate the values of respective NMR parameters for each of these conformers and to compare them to the measured NMR data, trying to determine the solution conformation(s) for the cyclic moieties of both peptides. We have calculated lower and upper limits of the $J_{HNC\alpha H}$ vicinal constant values of the HCys/Cys^3 and Tyr^4 residues for all conformers in Table 2, assuming possible fluctuations of ϕ_3 and ϕ_4 values as ±15° [see also Nikiforovich et al., (1993a)] and employing $J_{HNC\alpha H}(\phi)$ curves suggested by various authors (Bystrov, 1976; Demarco et al., 1978; Ludvigsen et al., 1991; Pardi et al., 1984). The calculated limits of $J_{HNC\alpha H}$ values consistent with the experimental data are listed in Table 5.

Table 5 clearly shows that the most distinctive parameter to distinguish among conformers of Table 4 is a high experimental value of the J(Tyr^4) coupling constant, which corresponds almost in all cases to the *D* type backbone conformer of the Tyr^4 residue, i.e., to structures 1, 4, 5, 7, 8, 10, and 11 for *cyclo*[Sar^1, HCys^3, Mpt^5]-AT and 1, 2, 3, 5, 8, and 9 for *cyclo*[Sar^1, Cys^3, Mpt^5]-AT. The only exception is structure 15 for *cyclo*[Sar^1, Cys^3, Mpt^5]-AT with *B* type conformation of Tyr^4; in this case, however, the ω angle between Tyr^4 and Mpt^5 is highly distorted from the *trans* conformation, which is not in accord with the high experimental NOE value between αH_{Tyr} and δH_{Mpt} (see above). The same backbone structure for the Tyr^4 residue was suggested by the models of solution conformations for both peptides derived directly from NMR data (see above).

To estimate the rotamer population for the Tyr^4 side chain, we have performed additional energy calculations for both cyclic peptides in question, considering all combinations of rotamers (g^+, t and g^-) for the side chains of the Tyr^4, His^6, and Phe^8 residues, rather than using the optimization algorithm mentioned under Materials and Methods. After energy minimization was completed, we have selected the conformers satisfying the $\Delta E \leq 10$ kcal/mol criterion and have counted the numbers of conformers with the χ_1(Tyr^4) values close to 60°, 180°, and −60° (± 40°). It appeared that these numbers were of 5% (3%) for g^+, 36% (40%) for t, and 59% (56%) for g^- rotamers of the Tyr^4 side chain in *cyclo*[Sar^1, Cys^3, Mpt^5]-AT (*cyclo*[Sar^1, HCys^3, Mpt^5]-AT), respectively, being in agreement with the rotamer population suggested by NMR (Table 2).

Thus, both NMR data and independent energy calculations lead to the same unique model for the conformation of cyclic moieties of *cyclo*[Sar^1, HCys^3, Mpt^5]-AT and *cyclo*[Sar^1, Cys^3, Mpt^5]-AT in solution (see Figure 3), despite all uncertainties inherent to the methods used (neglecting conformational averaging in NMR data, inaccuracy of the force field and solvent in the calculations). To our knowledge, it is the first

Table 6: Possible Models for Receptor-Bound Conformers of AT vs *cyclo*[Sar^1, HCys^3, Mpt^5]-AT and *cyclo*[Sar^1, Cys^3, Mpt^5]-AT (Only Fragments 4–8 Included)

	Tyr		Val/HCys/Cys		His		Pro		Phe
compound	ϕ	ψ	ϕ	ψ	ϕ	ψ	ϕ	ψ	ϕ
AT	−81	−32	−86	−35	−138	83	−60	64	−138
cyclo[Cys^3,Mpt^5]-AT	−130	56	−60	129	52	77	−60	74	−135
cyclo[HCys^3, Mpt^5]-AT	−133	70	−60	−13	−145	75	−60	67	−147

case of an unequivocal determination of a single conformation for a cyclic peptide moiety in solution; for instance, in the case of the just slightly more flexible DPDPE cycle (14-membered ring), several low-energy conformers were found to satisfy the NMR data (Nikiforovich et al., 1993a).

Possible Receptor-Bound Conformation(s). Since both cyclic analogs in question possess high level of binding to specific receptors, structures of Table 4 should include conformers compatible with AT receptor-bound conformer-(s). None of the *cyclo*[Sar^1, HCys^3, Mpt^5]-AT conformers in Table 4 displays β-turn-like features in positions 3–4 or 4–5. At the same time, 19 out of 382 low-energy *cyclo*[Sar^1, HCys^3, Mpt^5]-AT conformers show pronounced similarity to the model of AT receptor-bound conformation (Nikiforovich & Marshall, 1993), which assumes the particular spatial arrangement of aromatic moieties of Tyr^4, His^6, and Phe^8 residues and the C-terminal carboxyl (the rms values $\leq$1.0 Å, being compared according to Materials and Methods). All of these conformers share virtually the same structure of fragment 3–8, which includes the single type of backbone, namely, *F/E D A D C E* (the discussed model of receptor-bound conformation of AT requires backbone conformations of *A/E A D C E* type for fragment 4–8). Exactly the same is true for *cyclo*[Sar^1, Cys^3, Mpt^5]-AT conformers; in this case the similarity to the same model of AT receptor-bound conformation was shown by 43 structures out of 1331. The AT receptor-bound conformer in question (Nikiforovich & Marshall, 1993) is depicted in Figure 4 and is described in Table 6 along with compatible structures of *cyclo*[Sar^1, HCys^3, Mpt^5]-AT and *cyclo*[Sar^1, Cys^3, Mpt^5]-AT. Note that the β-III turn in the backbone of the Tyr^4-Val^5 residues in the receptor-bound conformation for AT itself is substituted by "an open turn" (Plucinska et al., 1993) for cyclo analogs, thus confirming the suggestion that the conformation(s) ensuring binding of AT analogs toward specific receptors should not be described in terms of backbone conformers (Nikiforovich & Marshall, 1993).

It is noteworthy also that among low-energy conformers of *cyclo*[Sar^1, HCys^3, Mpt^5]-AT and *cyclo*[Sar^1, Cys^3, Mpt^5]-AT possessing the backbone conformation of the D type for the Tyr^4 residue, required by solution conformations of cyclic moieties, there are three-dimensional structures which are similar to the model of AT receptor-bound conformation (see above). This finding suggests that the conformations of the cyclic moieties, which are the most rigid elements of *cyclo*[Sar^1, HCys^3, Mpt^5]-AT and *cyclo*[Sar^1, Cys^3, Mpt^5]-AT, are already prearranged in solution to be suitable for further receptor binding. It might be one another indirect indication in favor of the "induced fit" or "zipper" mechanism for an alteration of solution conformations of short peptides toward the receptor-bound conformers [see also Nikiforovich et al. (1993a,b)].

REFERENCES

Balodis, Y. Y., & Nikiforovich, G. V. (1980) *Bioorg. Khim. 6*, 865–875 (in Russian).

Bax, A., & Davis, D. G. (1985) *J. Magn. Reson. 65*, 355.

Bystrov, V. (1976) *Prog. Nucl. Magn. Reson. Spectrosc. 10*, 41.

Chipens, G. I., Ancan, Y. E., Nikiforovich, G. V., Balodis, Y. Y., & Makarova, N. A. (1979) in *Peptides-1978. Proceedings of the 15th European Peptide Symposium* (Siemion, I. Z., & Kupryszewski, G., Eds.) pp 415–419, Wroclaw University Press, Wroclaw, Poland.

De Coen, J.-L., Ralston, E., Durieus, J. P., & Loffet, A. (1975) in *Peptides: Chemistry, Structure and Biology*, pp 553–558, Pierce Co., Ann Arbor, MI.

de Leeuw, F. A. A. M., & Altona, C. (1982) *Int. J. Pept. Protein Res. 20*, 120.

Demarco, A., Llinas, M., & Wüthrich, K. (1978) *Biopolymers 17*, 637–650.

Deslauriers, R., Smith, I. C. P., & Walters, R. (1974) *J. Biol. Chem. 249*, 7006–7010.

Devynck, M.-A., Pernollet, M.-G., Meyer, P., Fermandjian, S., & Fromageot, P. (1973) *Nature, New Biol. 245*, 55–58.

Duncia, J. V., Chiu, A. T., Carini, D. J., Gregory, G. B., Johnson, A. L., Price, W. A., Wells, G. J., Wong, P. C., Calabrese, J. C., & Timmermans, P. B. M. W. M. (1990) *J. Med. Chem. 33*, 1312–1329.

Dunfield, L. G., Burgess, A. W., & Scheraga, H. A. (1978) *J. Phys. Chem. 82*, 2609–2616.

Fermandjian, F., Lintner, K., Haar, W., Fromageot, P., Khosla, M. C., Smeby, R. R. & Bumpus, F. M. (1976) in *Peptides-1976* (Loffet, A., Ed.) pp 514–525, University of Brussel, Bruxelles, Belgium.

Kessler, H., Bermel, W., Friedrich, A., Krack, G., & Hull W. E. (1982) *J. Am. Chem. Soc. 104*, 6297.

Kessler, H., Griesinger, C., Kerssebaum, R., Wanger, K., & Ernst, R. R. (1987) *J. Am. Chem. Soc. 109*, 607.

Ludvigsen, S., Andersen, K. V., & Poulsen, F. M. (1991) *J. Mol. Biol. 217*, 731–736.

Marshall, G. R. (1986) *Dtsch. Apoth. Ztg. 126*, 87–90.

Matsoukas, J. M., Bigam, G., Zhou, N., & Moore, G. J. (1990) *Peptides 11*, 359–366.

Miranda, A., & Juliano, L. (1988) *Braz. J. Med. Biol. Res. 21*, 903–914.

Nemethy, G., Pottle, M. S., & Scheraga, H. A. (1983) *J. Phys Chem 87*, 1883–1887.

Nikiforovich, G. V., & Marshall, G. R. (1993) *Biochem. Biophys. Res. Commun. 195*, 222–228.

Nikiforovich, G. V., Vesterman, B. G., & Betins, J. (1988) *Biophys. Chem. 31*, 101–106.

Nikiforovich, G. V., Hruby, V. J., Prakash, O., & Gehrig, C. A. (1991) *Biopolymers 31*, 941–955.

Nikiforovich, G. V., Prakash, O., Gehrig, C., & Hruby, V. J. (1993a) *Int. J. Pept. Protein Res. 41*, 347–361.

Nikiforovich, G. V., Prakash, O., Gehrig, C. A., & Hruby, V. J. (1993b) *J. Am. Chem. Soc. 115*, 3399–3406.

Paiva, T. B., Paiva, A. C. M., & Scheraga, H. A. (1963) *Biochemistry 2*, 1327–1334.

Pardi, A., Billeter, M., & Wüthrich, K. (1984) *J. Mol. Biol. 180*, 741–751.

Plucinska, K., Kataoka, T., Yodo, M., Cody, W. L., He, J. X., Humblet, C., Lu, G. H., Lunney, E., Major, T. C., Panek, R. L., Schelkun, P., Skeean, R., & Marshall, G. R. (1993) *J. Med. Chem. 36*, 1902–1913.

Printz, M. P., Nemethy, G., & Bleich, H. (1972) *Nature, New Biol. 237*, 135.

Roterman, I. K., Lambert, M. H., Gibson, K. D., & Scheraga, H. A. (1989) *J. Biomol. Struct. Dyn. 7*, 421–453.

Smeby, R. R., Arakawa, K., Bumpus, F. M., & Marsch, M. M. (1962) *Biochim. Biophys. Acta 58*, 550–557.

Spear, K. L., Brown, M. S., Reinhard, E. J., McMahon, E. G., Olins, G. M., Palomo, M.A., & Patton, D. R. (1990) *J. Med. Chem. 33*, 1935–1940.

Sugg, E. E., Dolan, C. A., Patchett, A. A., Chang, R. S. L., Faust, K. A., & Lotti, V. J. (1989) *Proceedings of 11th American Peptide Symposium*, 305–306.

Turner, R. J., Matsoukas, J. M., & Moore, G. J. (1991) *Biochim. Biophys. Acta 1065*, 21–28.

Weinkam, R. J., & Jorgensen, E. C. (1971) *J. Am. Chem. Soc. 93*, 7033–7038.

Wüthrich, K., Billeter, M., & Braun, W. (1984) *J. Mol. Biol. 180*, 715.

Zimmerman, S. S., & Scheraga, H. A. (1977) *Biopolymers 16*, 811–843.